A Numerical Study of a Nonstationary Solution of the Hasselmann Equation

IGOR V. LAVRENOV

State Research Center of the Russian Federation, Arctic and Antarctic Research Institute, St. Petersburg, Russia

(Manuscript received 18 June 2001, in final form 30 July 2002)

ABSTRACT

The Hasselmann kinetic equation describing nonlinear spectrum evolution of gravity surface waves is investigated for their large periods of time. To solve the problem, the most optimal numerical algorithm of the nonlinear energy transfer computation is used. The nonlinear spectrum evolution is described by various features. The numerical results reveal some general details common for all cases of the spectrum evolution. There are two main domains in the spectrum: a sharply defined peak and a slowly decreasing high-frequency tail. Using the numerical results, an intermediate self-similar frequency spectrum asymptotic approximation is proposed. It is confirmed by field observations of swell spectrum propagating at large distances. This approximation describes the main features of the nonlinear spectrum evolution and provides a preservation of the total energy and wave action.

1. Introduction

Modern wind-wave models are based on the numerical solution of the energy balance equation. Its right-hand side describes different physical mechanisms forming the wind-wave spectrum (Davidan et al. 1985; Komen et al. 1994). There are at least three physical mechanisms: wind-wave energy input, energy dissipation, and nonlinear energy transfer. In the case of swell propagating from distant storms (i.e., from a wind-wave generation area), a dissipation of the low-frequency swell is so small that it can propagate at global distances without losing any essential energy (Snodgrass et al. 1966; Lavrenov and Pasechnik, 1989). That is why energy dissipation can be neglected in the energy balance equation in numerical simulation of swell propagation. There are two main factors of swell spectrum formation in the ocean: wave energy divergence and nonlinear energy transfer. The divergence caused by wave propagation is described by an advective term in the left-hand side of the energy balance equation. The swell length and period become larger in wave propagation due to dispersion. As for the nonlinear swell evolution, it remaines less investigated. Its mechanism is supposed to be of less importance because of small wave steepness, which is a parameter of nonlinearity. However, in reality it is not quite so. Because of large time of swell propagation in the ocean, the nonlinearity can influence swell spectrum formation. So, the time of swell propagation at the large distance L is estimated as $T = L/C_g$, where C_g is a wave group velocity. In the case of swell propagation in the ocean, the value of L is estimated as $\approx 10^7$ m. For the wave period $\tau \approx 10$ s, the group velocity is estimated as $C_g = g\tau/4\pi \approx 10$ m s^{-1}, where g is gravitational acceleration. It means that $T = 10^6$ s. Note that it is enough time to produce a nonlinear effect on swell spectrum formation. According to the field data (Davidan et al. 1985), the swell frequency spectrum can be approximated as follows: $S(\sigma) \approx m_0(n + 1)(\sigma_p/\sigma)^n\ 1/\sigma/\ \exp[(n + 1/n)(\sigma_p/\sigma)^n]$, where m_0 is a zero moment of the spectrum, σ is a frequency, σ_p is a frequency of the spectrum maximum, and n is estimated as ≥ 5. The spectrum can be approximated as $S(\sigma) \sim 1/\sigma^{n+1}$ for $\sigma > \sigma_p$. So, despite wave dispersion and dissipation, the swell spectrum preserves some stable form, which could be controlled by nonlinear energy transfer in the wave spectrum. To clarify this problem, it would be interesting to estimate this effect by numerical simulation of the kinetic equation, describing wave spectrum evolution by nonlinear energy transfer.

For the first time the problem of the nonlinear energy transfer in the wind-wave spectrum was formulated by Hasselmann (1962, 1963) and Zakharov (1968). According to their theory, the nonlinear evolution of the wave action is described by the following kinetic equation:

Corresponding author address: Igor V. Lavrenov, State Research Center of the Russian Federation, Arctic and Antarctic Research Institute, Bering 38, St. Petersburg 199397, Russia.
E-mail: lavren@aari.nw.ru

$$\frac{\partial N(\mathbf{k})}{\partial t} = \iiint T(\mathbf{k}, \mathbf{k}_1, \mathbf{k}_2, \mathbf{k}_3)\delta(\mathbf{k} + \mathbf{k}_1 - \mathbf{k}_2 - \mathbf{k}_3)\delta(\sigma + \sigma_1 - \sigma_2 - \sigma_3) \times [N_2N_3(N + N_1) - N_1N(N_2 + N_3)]\, d\mathbf{k}_1\, d\mathbf{k}_2\, d\mathbf{k}_3, \tag{1}$$

TABLE 1. Values of the initial spectrum parameters.

	$2s = 2$		$n_\beta = 2$		$n_\beta = 8$	
γ	B	D_p	B	D_p	B	D_p
1.0	0.69	0.32	0.69	0.64	0.69	1.16
3.3	0.34	0.32	0.34	0.64	0.34	1.16
7.0	0.25	0.32	0.25	0.64	0.25	1.16

where $N_i = N(\mathbf{k}_i)$ is a spectral density of wave action, $T(\mathbf{k}, \mathbf{k}_1, \mathbf{k}_2, \mathbf{k}_3)$ are matrix elements of four-resonance-wave interaction, and $\delta(\mathbf{k})$ and $\delta(\sigma)$ are delta functions. They describe the resonance condition between the four wave components:

$$\mathbf{k} + \mathbf{k}_1 = \mathbf{k}_2 + \mathbf{k}_3, \quad \text{and} \tag{2a}$$

$$\sigma + \sigma_1 = \sigma_2 + \sigma_3, \tag{2b}$$

The main peculiarity of Eq. (1) is a preservation of the following quantities:

total wave action,

$$A = \int N(\mathbf{k})\, d\mathbf{k}, \tag{3a}$$

total energy,

$$E = \int \sigma N(\mathbf{k})\, d\mathbf{k}, \tag{3b}$$

and total momentum,

$$\mathbf{K} = \int \mathbf{k}N(\mathbf{k})\, d\mathbf{k}. \tag{3c}$$

Hasselmann proved the existence of the integral in Eq. (3) in 1965.

Later on, the algorithm elaboration of the collision integral estimation in Eq. (1) was carried out for the study of nonlinear energy transfer. So, some effective numerical schemes were worked out, and the main integral features were investigated in papers (Hasselmann and Hasselmann 1981, 1985; Komen et al. 1994; Komatsu and Masuda 1996; Masuda 1980, Lavrenov 1991a,b, 1998, 2001; Lavrenov and Ocampo-Torres 1999; Polnikov 1989, 1990, 1993; Resio and Perrie 1991; Snyder et al. 1993; Webb 1978, etc.).

However, still not enough attention has been paid to the problem of analytical and numerical study of the kinetic Eq. (1) as it is. Among the stationary analytical solutions the following one is known as ‘‘thermodynamical’’:

$$N = (a + b\sigma + c\mathbf{k})^{-1}, \tag{4}$$

where a, b, and c are constants. The solution in Eq. (4) reduces the integral value to zero. However, it is not of much physical interest when its small disturbances lead to divergence of the integral value in Eq. (1).

The investigation of the equation solution in Eq. (1) still remains an important and difficult problem. The main progress in its analytical study was achieved by Zakharov and Filonenko (1966), Zakharov and Smilga (1981), and Zakharov and Zaslavskii (1982, 1983). A solution of the stationary analytical spectra of Eq. (1) was derived for the angle isotropic case and the infinite frequency range $[0, \infty]$. In cases in which wave energy input and dissipation are very widely separated, the wave spectrum is approximated by the Kolmogorov–Zakharov dependence. Analytical methods of the equation solution were developed further in papers (Zaslavskii 1989, 2000) based on the ‘‘narrow directional approximation.’’ According to Zaslavskii (2000), a solution of Eq. (1) can be presented as a self-similar form. The frequency spectral dependence is found out to be equal to $S(\sigma) \sim \sigma^{-13/2}$ (for $\sigma > \sigma_p$, where σ_p is a peak spectrum frequency), frequency spectral maximum evolution is estimated as $\sigma_p \sim t^{-1/11}$, and angular narrowness in the vicinity of the spectral maximum is $D_p \cong 1$. However, the simplified equations used by Zaslavskii (2000) unfortunately do not provide a complete picture of the whole evolution equation. His self-similar spectrum approximation does not satisfy the energy preservation law.

Note that there are not many papers devoted to the problem of the numerical simulation of Eq. (1). In Polnikov (1990, 1999), it is shown that the solution is not dependent on the initial spectral form and the integral spectral parameters are varied within narrow bands for a large timescale of the nonlinear evolution. The effect is considered to be an establishing one of the self-similar spectral form and is confirmed by analytical estimations (Zaslavskii 2000).

The problem of a self-similar solution seemed to have been solved. However, in Komatsu and Masuda (1996) the numerical solutions are different from the results of Polnikov (1990) and Zaslavskii (2000). The difference is not only in another spectral tail frequency dependence, but also in the integral parameters. So, the numerical result provides the following approximation $S(\sigma) \sim \sigma^{-4}$ (for $\sigma > 1.5\sigma_p$). The problem still remains unsolved, and it can be formulated in such a way: is there an exact self-similar form of the spectrum? And then: if the answer is positive, what are the values of its parameters?

An attempt is undertaken here to solve the problem.

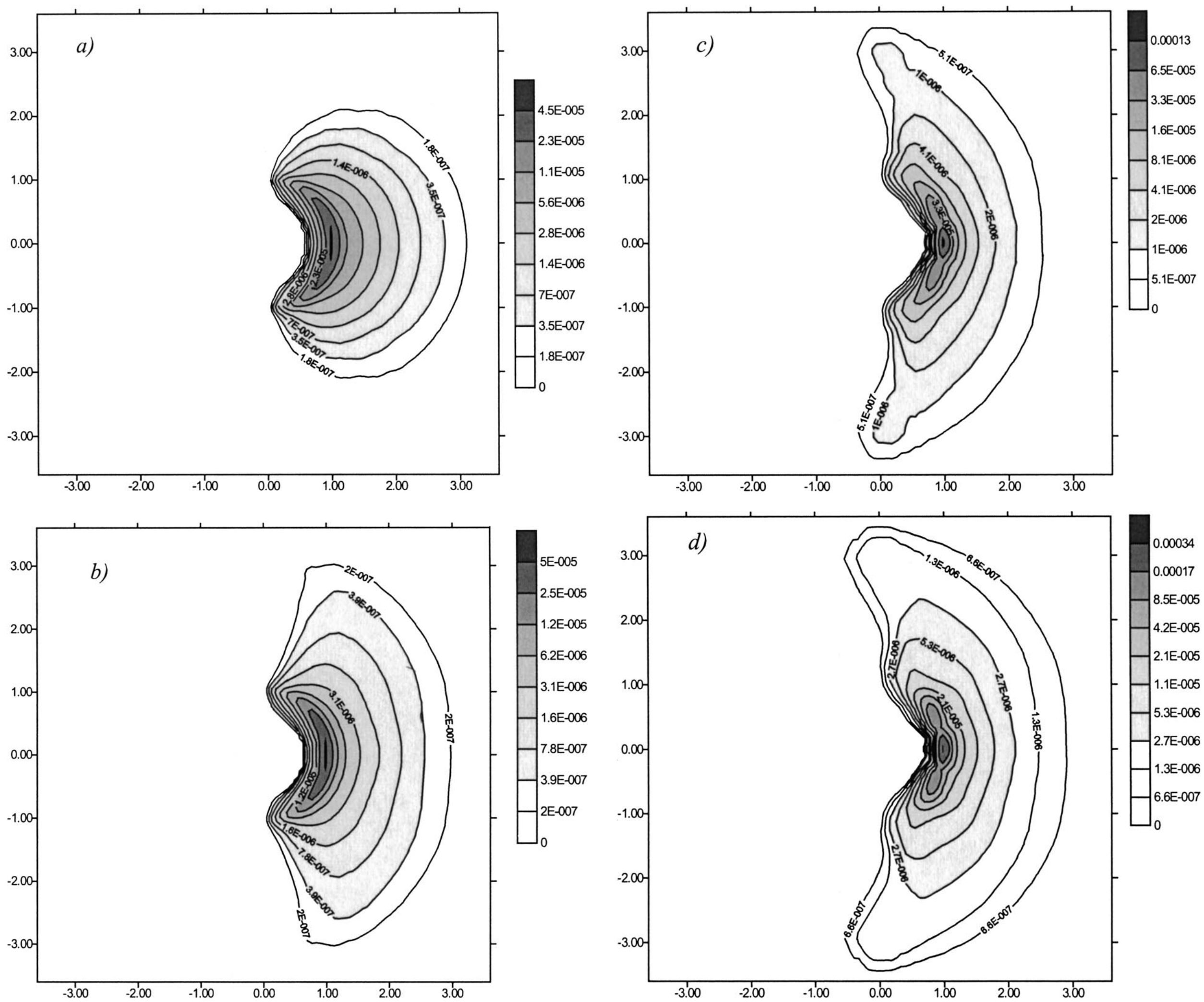

FIG. 1. Nonlinear two-dimensional spectrum evolution with the initial spectrum values of Eqs. (10) and (11) and $\gamma = 3.3$ and $n = 2$ at different time moments: $\tilde{t}$ = (*a*) 0, (b) 10^3, (c) 10^5, and (d) 10^7.

This paper contains the following sections: a timescale of nonlinear spectrum evolution is considered in section 2. The numerical results for the nonisotropic spectrum are presented in section 3. A problem of self-similar frequency spectrum approximations is discussed in section 4. Comparison between theoretical and experimental results is discussed in section 5.

2. Timescale of establishing self-similar solution

In this paper, the timescale T of spectral nonlinear evolution is considered as a value on which the nonlinear energy transfer exchanges fully its spectral form. It should not depend on the initial spectrum details. To estimate the timescale T, the total wave action [Eq. (3a)] is divided by an effective value of the action flux F_n. The latter is determined by the preservation law of the total wave action:

$$\frac{\partial N(\mathbf{k})}{\partial t} + \mathrm{div}_{\mathbf{k}}\mathbf{F}_n = 0, \tag{5}$$

where $\mathbf{F}_n$ is a vector of the action flux. According to Polnikov (1999), the T value can be estimated with the help of the ratio of the spectral maximum N_p to a maximum of the nonlinear transfer $(\partial N/\partial t)_p$:

$$T \cong N_p/(\partial N/\partial t)_p. \tag{6}$$

To get the estimation T, one can transfer from the wave action spectrum $N(\mathbf{k})$ to frequency–angular spectrum $S(\sigma, \beta)$ using the formula

$$N(\mathbf{k})d\mathbf{k} \propto \frac{1}{\sigma}S(\mathbf{k})d\mathbf{k} \propto \frac{g^3}{2\sigma^4}S(\sigma, \beta)d\sigma d\beta, \tag{7}$$

where $\sigma^2 = gk$ is a deep-water dispersion relation. For the typical values $\sigma_{\max} = 1$ rad s^{-1} and $S_{\max} = 0.2$ m^2 s, it is possible to obtain

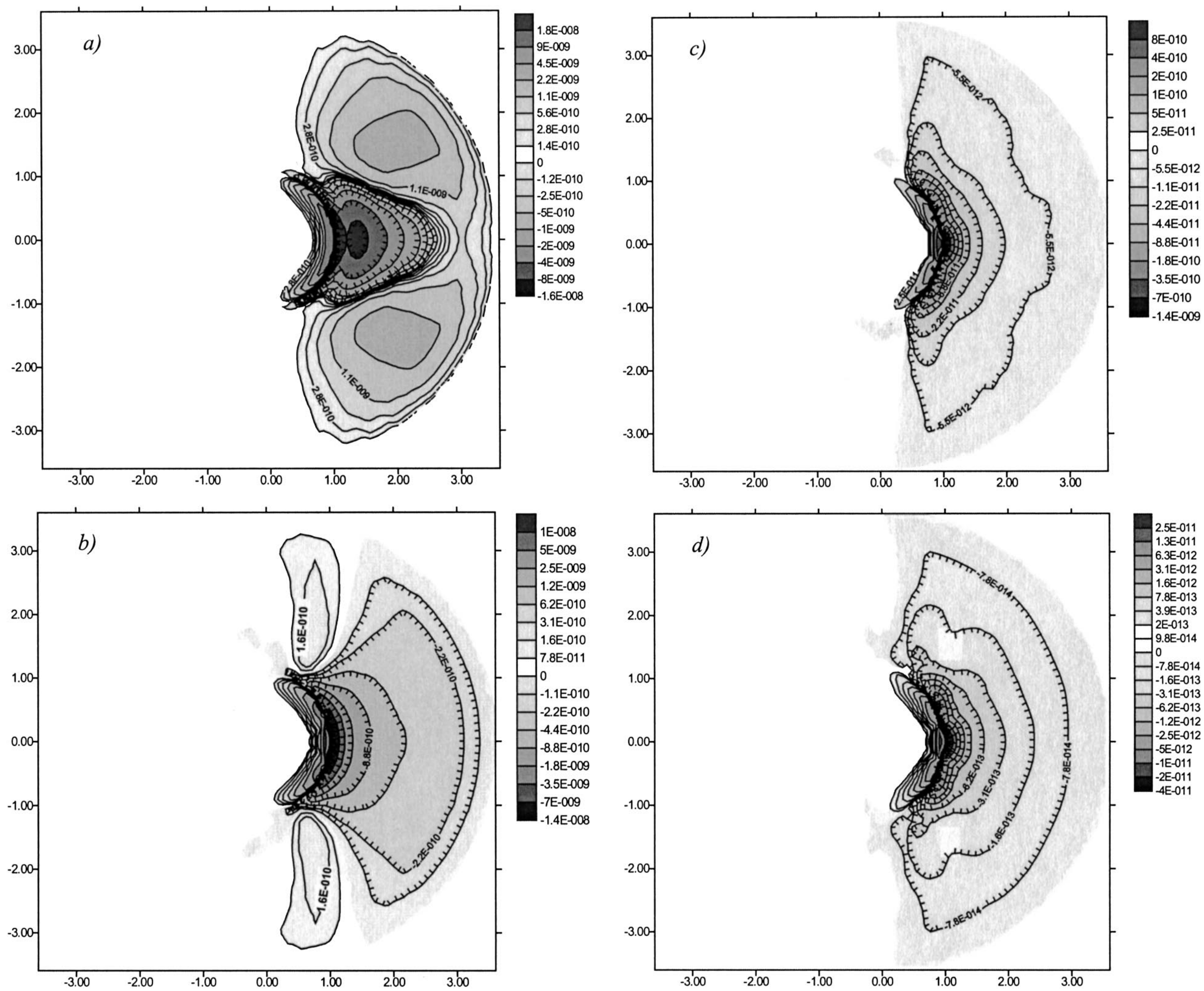

FIG. 2. Same as Fig. 1, but for two-dimensional nonlinear energy transfer function evolution.

$$T \cong 10^5\tau, \tag{8}$$

where $\tau = 2\pi/\sigma_{\max}$ is a period of the initial spectral maximum.

Thus, a nonlinear evolution establishing self-similar spectral form happens at a timescale larger than the estimation in Eq. (8): $\tilde{t} = t/\tau > T/\tau$.

3. Nonlinear evolution of JONSWAP spectrum

a. Initial conditions

Nonlinear energy spectrum evolution should be computed for the most typical initial frequency–angular approximations $S(\sigma, \beta)$, such as

$$S(\sigma, \beta) = S(\sigma)Q(\sigma,\beta), \tag{9}$$

where $S(\sigma)$ is the frequency spectrum and $Q(\sigma, \beta)$ is the angular distribution.

The frequency approximation is used in the form of the Joint North Sea Wave Project (JONSWAP) spectrum (Hasselmann et al. 1973):

$$S(\sigma) = \alpha g^2\sigma^{-5} \exp\left[-\frac{5}{4}\left(\frac{\sigma_{\max}}{\sigma}\right)^4\right] \times \gamma^{\exp[-(\sigma-\sigma_{\max})^2/(2\sigma_J^2\sigma_{\max}^2)]}, \tag{10}$$

where

$$\sigma_J = \begin{cases} 0.07 & \text{at } \tilde{\sigma} \le 1; \\ 0.09 & \text{at } \tilde{\sigma} > 1; \end{cases} \qquad \tilde{\sigma} = \frac{\sigma}{\sigma_{\max}},$$

with $\sigma_{\max}$ being a frequency of spectrum maximum of the initial spectrum.

The energy angular distribution is used consecutively in the form of two approximations, one of them being an ordinary cosine energy dependence:

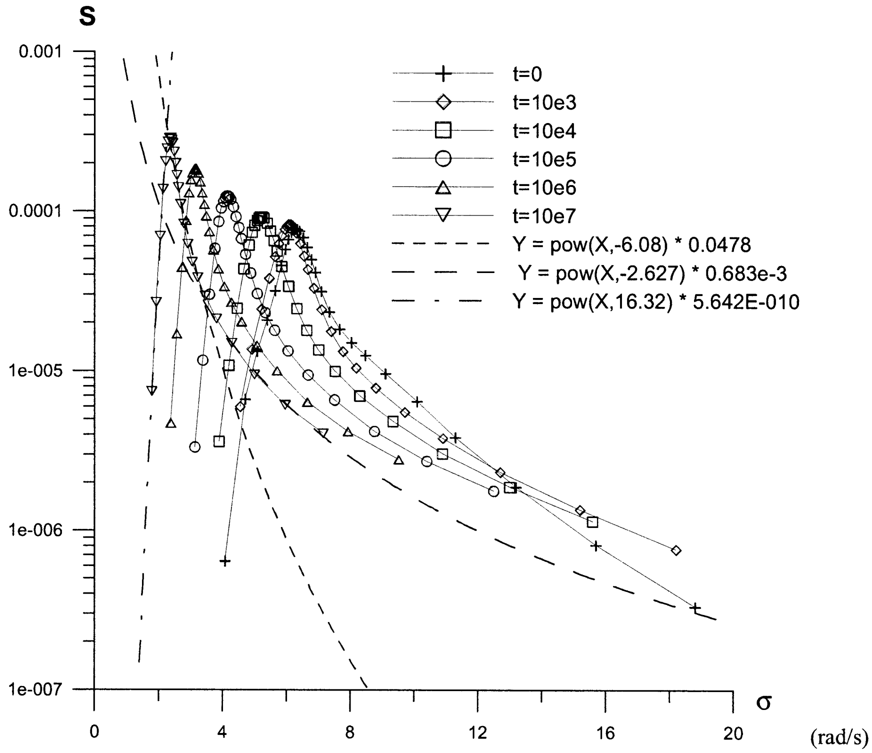

FIG. 3. Frequency spectrum evolution with the initial values of Eqs. (10) and (11) and $\gamma = 3.3$ and $n = 2$ at different time moments.

$$Q(\sigma, \beta) = \begin{cases} \left[\dfrac{\pi\Gamma(n_\beta + 1)}{2^{n_\beta}\Gamma^2(n_\beta/2 + 1)}\right]^{-1} \cos^{n_\beta}(\beta - \overline{\beta}) \\ \quad \text{at } |\beta - \overline{\beta}| \le \pi/2 \\ 0 \quad \text{at } |\beta - \overline{\beta}| \ge \pi/2, \end{cases} \tag{11}$$

where $\overline{\beta}$ is mean (or general) direction of wave propagation.

The second angular distribution is used in the following form:

$$Q_J(\sigma, \beta) = \left[\frac{2^{2s-1}\pi\Gamma^2(s + 1)}{\Gamma(2s + 1)}\right] \cos^{2s}\left[\frac{(\beta - \overline{\beta})}{2}\right], \tag{12}$$

Nonlinear energy spectrum evolution is computed for these initial frequency–angular approximations $S(\sigma, \beta)$. In the process of computation the following parameters are estimated: the frequency width B, defined as

$$B = \int S(\sigma)\, d\sigma/S(\sigma_p)\sigma_p, \quad \text{and} \tag{13}$$

the directional width D, defined as

$$D(\sigma) = S(\sigma, \overline{\beta})/S(\sigma), \tag{14}$$

where $S(\sigma) = \int_{-\pi}^{\pi} S(\sigma, \beta) d\beta$ and σ_p is a frequency of spectrum maximum, evaluated in time.

Series of the initial spectrum parameters γ, n_β, and $2s$ and initial values B and D defined at the general direction $D_p = D(\sigma_p) = S(\sigma_p, \overline{\beta})/S(\sigma_p)$ are presented in Table 1.

b. Numerical algorithm

Establishment of a self-similar spectral form, controlled by the nonlinear energy transfer, requires producing computations for a timescale larger than the estimation in Eq. (8) by at least one or two orders of magnitude: $\tilde{t} = t/\tau > 10^5$. The main problem is that the numerical computation of the integral in Eq. (1) takes much CPU time. It means that an algorithm of nonlinear energy transfer computations should be very fast. To solve the evolution equation, the integral in Eq. (1) must be computed thousands of times to reach the estimated timescale of spectrum evolution. That is why the most optimal algorithm is used in this study. Lavrenov (1991b, 1998, 2001) developed such an algorithm with the help of the numerical method of integration of the highest precision. The algorithm provides accurate results using relatively little CPU time.

A numerical solution of Eq. (1) is carried out using the semi-implicit method (WAMDI Group 1988; Lavrenov 1998). It should be noted that a traditional method of numerical integration usually leads to nu-

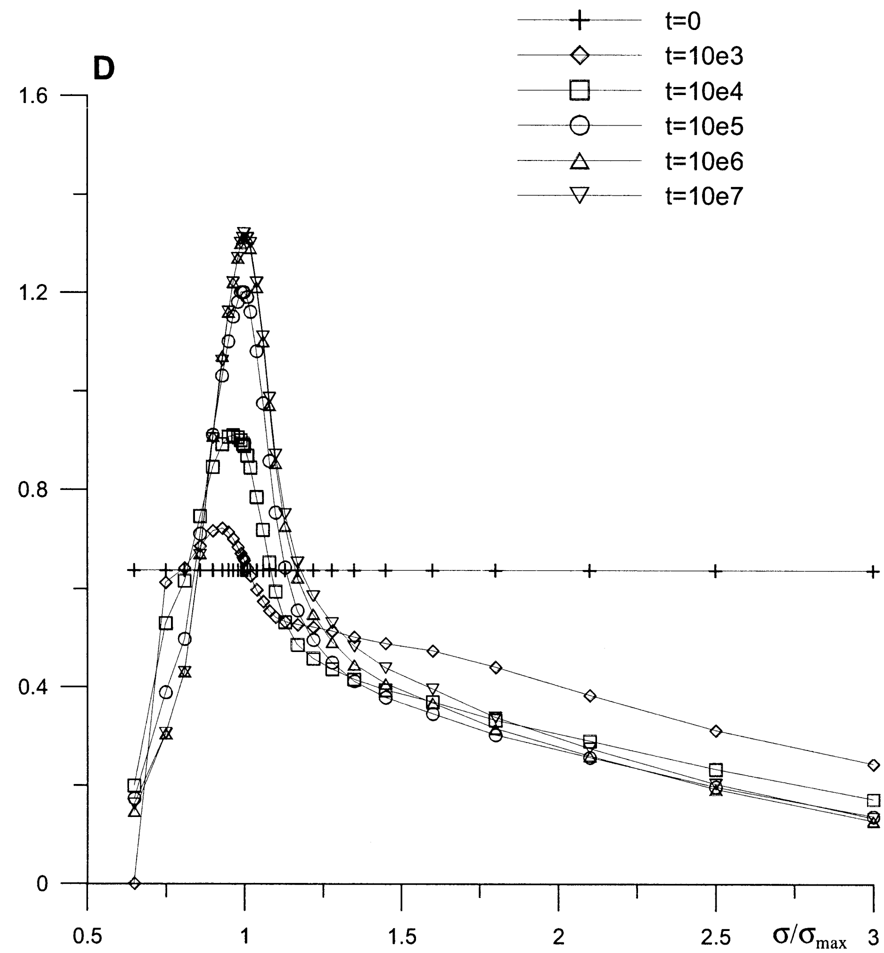

FIG. 4. Same as Fig. 3, but for the evolution of parameter *D*.

merical instabilities at the high-frequency spectral range. It requires a use of a small time step of numerical integration and special limits on a numerical solution and on a value of the source function (Lavrenov 1998; Tolman 1992). These methods unfortunately can violate energy preservation, leading to misinterpretation of physical results. However, a utilization of the semi-implicit numerical method does not produce any instabilities for relatively large time steps of numerical integration (Lavrenov 1998), and there is no need to use any limits.

The numerical accuracy and the preservation of the main integrals in Eq. (3) are controlled in the process of computation. So, a numerical error of the total energy preservation does not exceed 10% and the error of the total momentum estimation does not exceed 25% in comparison with its initial values.

c. Numerical results

Numerical results for initial conditions of Eqs. (10)–(11) with $\gamma = 3.3$ and $n = 2$ for four different time moments, $\tilde{t} \cong 0, 10^3, 10^5$, and 10^7, respectively, are presented in Figs. 1–4. Numerical simulation results of the relative frequency–angular spectrum values in the polar coordinate system, where a radius vector is a relative frequency value $\tilde{\sigma} = \sigma/\sigma_p$, are presented in Figs. 1a–d. The spectrum time evolution, resulting in a moonlike form, is shown. The spectrum becomes more narrow in the vicinity of the spectral maximum and wider at the high- and low-frequency range.

Two-dimensional nonlinear transfer values for the same steps of wave evolution are presented in Figs. 2a–d. The nonlinear evolution changes the spectrum form, shifting frequency of spectrum maximum to lower-frequency range. The nonlinear energy transfer function is changed to a larger extent in comparison with the spectrum. It becomes narrower with concentration intensity in the vicinity of the spectral maximum.

The frequency spectrum for the same evolution time steps is presented in Fig. 3. The spectrum is proportional to about $\sigma^{16.3}$ at the low-frequency range $\sigma_p > \sigma$ and it is proportional to about $\sigma^{-6.1}$ within the range $\sigma_p <$

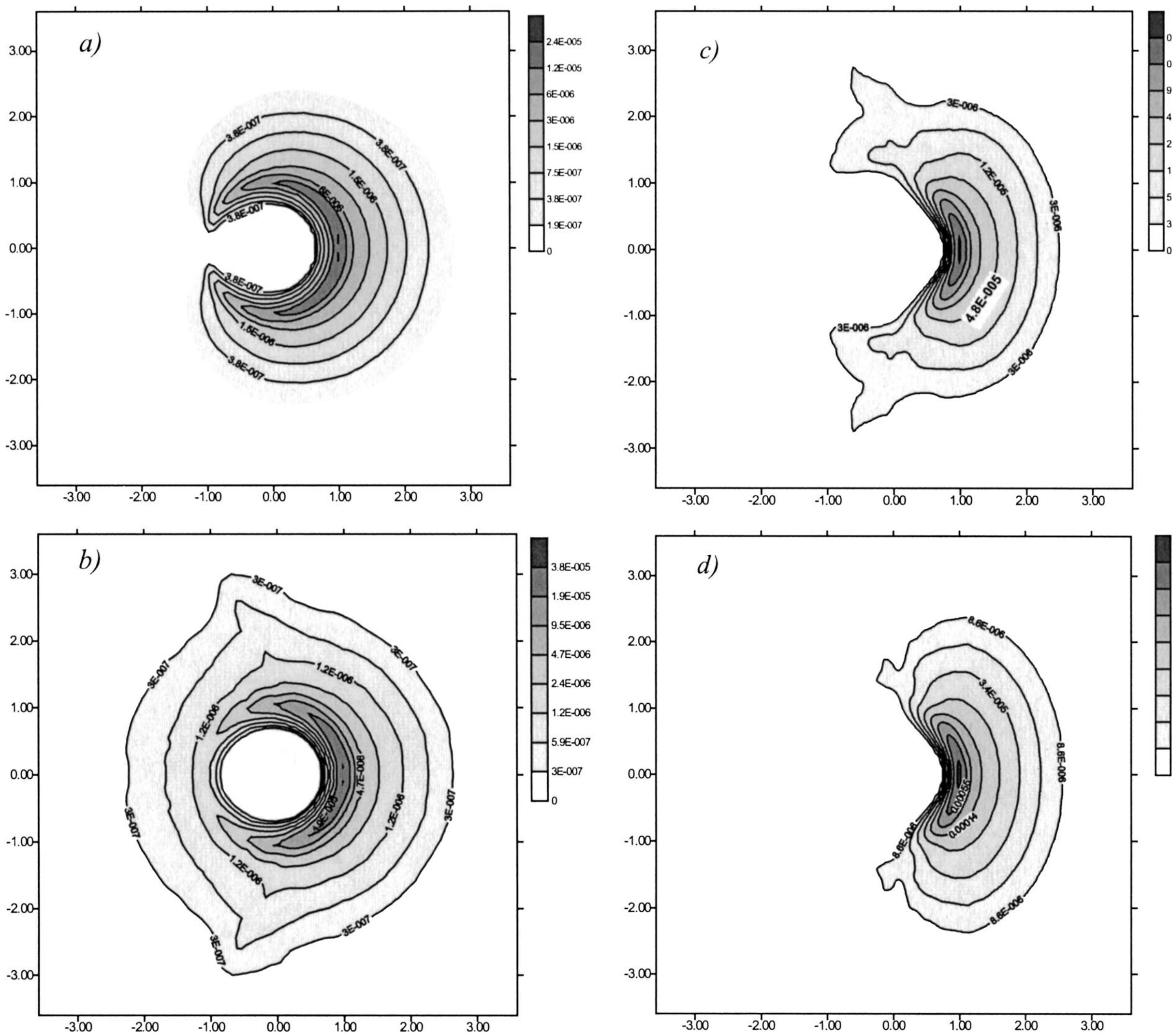

FIG. 5. Nonlinear two-dimensional spectrum evolution with the initial values of Eqs. (10) and (12) and $\gamma = 3.3$ and $2s = 2$ at different time moments: $\tilde{t} =$ (*a*) 0, (b) 10^3, (c) 10^6, and (d) 10^7.

$\sigma < 1.5\sigma_\pi$ (where $\sigma_\pi \approx 1.5\sigma_p$). The spectrum decreases as about $\sigma^{-2.6}$ at the larger frequencies $\sigma > \sigma_\pi$.

An evolution of the parameter D[Eq. (14)] for different time moments is presented in Fig. 4. The parameter D becomes larger and is equal to 1.33 in the vicinity of the spectral maximum, and it gets smaller at low- and high-frequency ranges. It is evidence of spectral isotropization within these frequency ranges.

The similar results for the initial frequency–angular spectrum of Eqs. (10) and (12) with $\gamma = 3.3$ and $2s = 2$ for the following steps of evolution: $\tilde{t} \cong 0$, 10^4, 10^6, and 10^7 are presented in Figs. 5–8. It is interesting to note that at the time moment $\tilde{t} \leq 10^4$ the frequency–angular spectrum (see Fig. 5) is varied and it becomes more isotropic as mentioned in Lavrenov and Ocampo-Torres (1999). It becomes more smooth and round. However, later on (at $\tilde{t} \geq 10^5$) it is transformed into a more directional form. The two-dimensional spectra could not become isotropic, as follows from the total momentum preservation law of Eq. (3c). So, the previous suggestion about the spectrum becoming isotropic with initial angular approximation [Eq. (12)] is disproved. The spectrum becomes more narrow in the vicinity of its maximum and is wider at low and high frequencies.

An important feature of the nonlinear energy transfer (see Fig. 6) is the presence of an area with positive values at the direction opposite to the main one of the wave propagation. Because of the action of the nonlinear energy transfer, the spectrum becomes more isotropic at the first stages of the evolution. Later on, this nonlinear energy transfer positive area disappears, with the spectrum becoming more directional and moving to the low-frequency range.

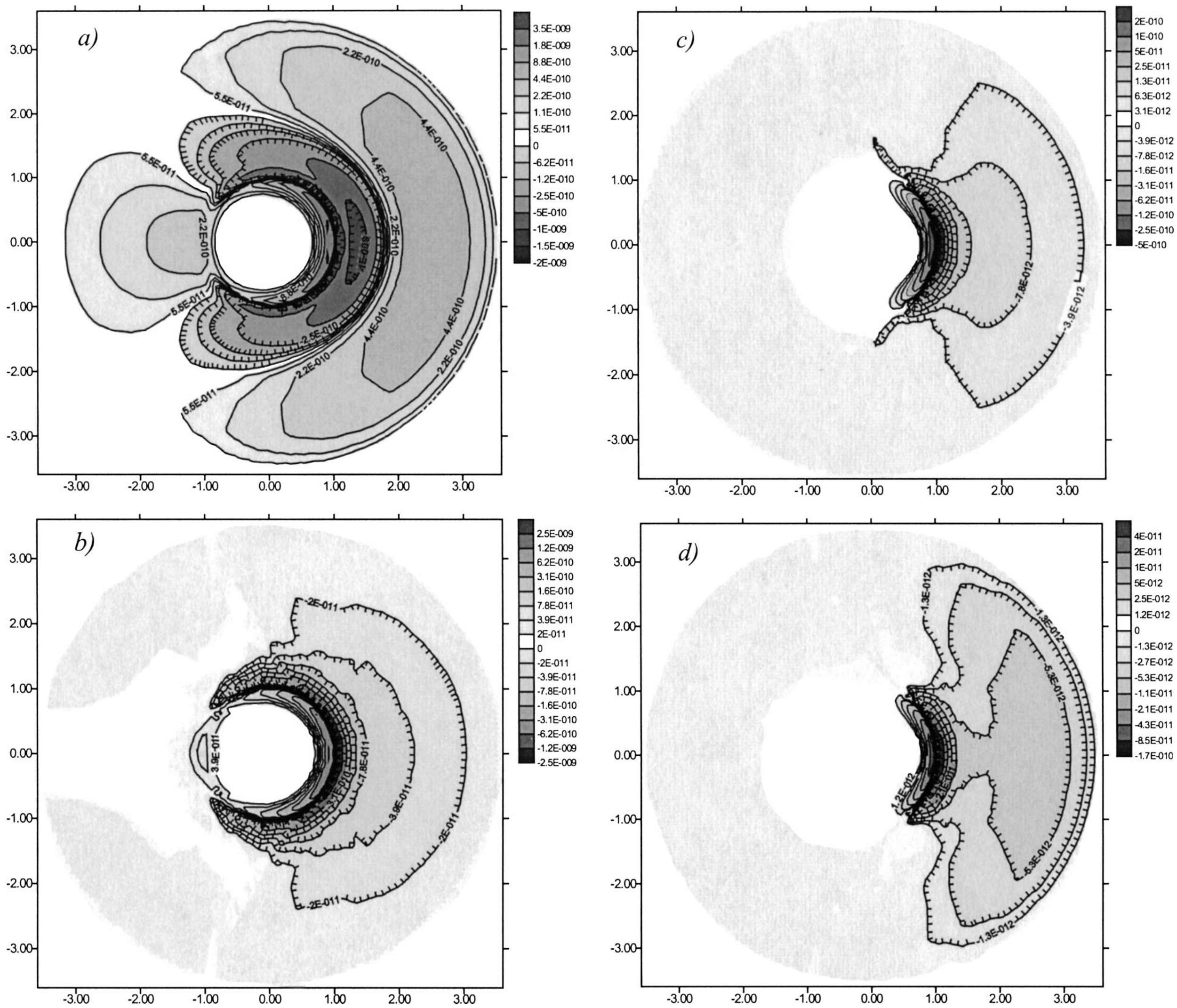

FIG. 6. Same as Fig. 5, but for two-dimensional nonlinear energy transfer function evolution.

The frequency spectrum is proportional to $S \sim \sigma^{17.0}$ at the low-frequency range $\sigma_p > \sigma$ (see Fig. 7). The spectrum is proportional to $\sim\sigma^{-6.2}$ within the range $\sigma_p < \sigma < \sigma_\pi$. It decreases as $\sim\sigma^{-3.67}$ at the high-frequency range, similar to the isotropic power spectrum. The function D (see Fig. 8) describing the angular narrowness is increased in the vicinity of the spectral maximum as is seen in the previous case (see Fig. 4), its value is smaller.

The numerical solutions for all initial spectra (see Table 1) are obtained for time duration up to $\tilde{t} = 10^7$–10^8. Results are presented in Table 2. The frequency of spectrum maximum evolution $\sigma_p = \sigma_p(t)$ for all these cases is presented in Fig. 9. The frequency of spectrum maximum shifts to the lower-frequency ranges as follows: $\sigma_p(t) \sim t^{-0.11}$. Time evolution of the parameter $B = B(t)$ for all initial conditions is presented in Fig. 10. The most important feature of the parameter $B = B(t)$ is the fact that it approaches to the same similar value for all initial conditions. It is approximately equal to $B \approx 1/3$. (the ''law of 1/3''). As shown by the numerical results, not only the parameter B, but also the parameter D_p, approaches to some constant value for all initial spectra. The digital final values of the parameters B and D_p for all initial spectra conditions are presented in Table 2.

4. Intermediate self-similar frequency spectrum asymptotic approximation

As shown by the numerical result, the spectrum reveals itself as a self-similar solution at large time of its nonlinear evolution. From this result, one can assume that the frequency spectrum does not depend on the features of the initial spectrum but should depend on the frequency of spectrum maximum σ_p, transition frequency from main frequency domain to high-frequency

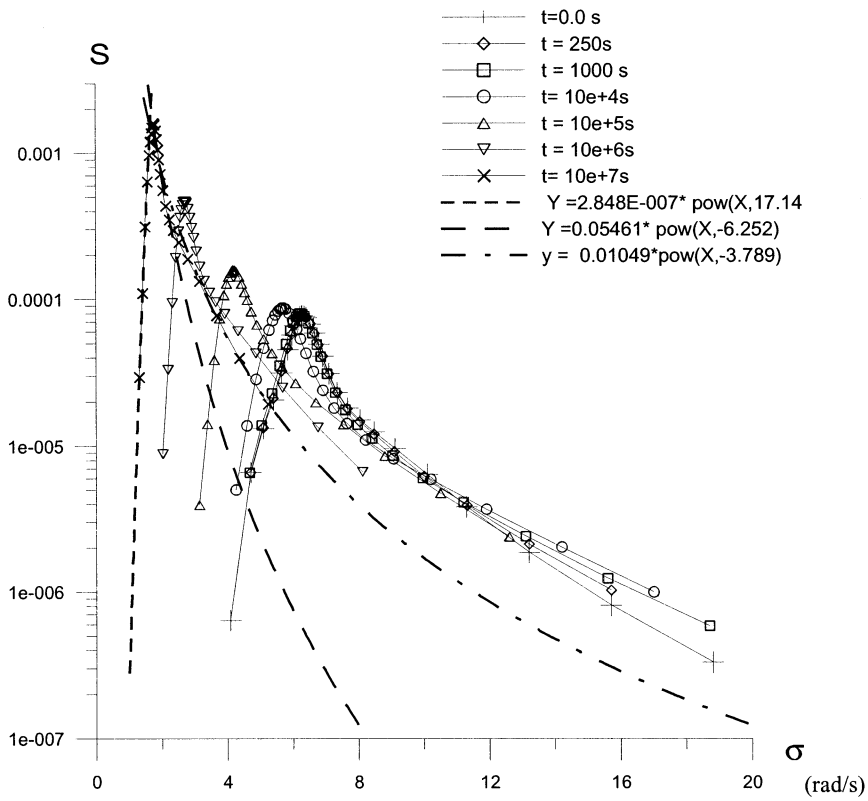

FIG. 7. Frequency spectrum evolution with the initial values of Eqs. (10) and (12) and γ = 3.3 and $2s$ = 2 at different time moments.

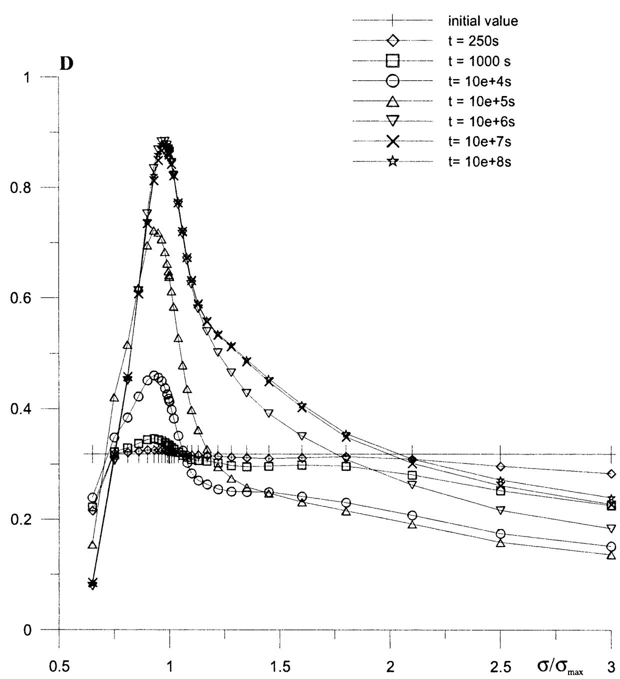

FIG. 8. Evolution of the parameter D in time with the initial values of Eqs. (10) and (12) and γ = 3.3 and n = 2 at different time moments.

range σ_π, time t, total energy E, and wave action A. Thus, the frequency spectrum S can be presented as a function of these parameters:

$$S = S(\sigma, \sigma_p, \sigma_\pi, t, E, A). \tag{15}$$

Using the Π theorem (Barenblatt 1984), it is possible to define a self-similar approximation as a function of four nondimensional parameters in the following form:

$$\frac{\sigma S(\sigma)}{E} = F\left(\frac{\sigma}{\sigma_p}, \frac{\sigma}{\sigma_\pi}, t\sigma_p, \frac{A\sigma_p}{E}\right), \tag{16}$$

where F is a function to be defined. It describes the main features of the obtained numerical solutions.

The number of variables in Eq. (16) can be diminished using the dependence between frequency of spectrum maximum and time $\sigma_p = \sigma_p(t)$. To satisfy the numerical results, the function F can be defined in the following way:

TABLE 2. Final values of the parameters B and D_p for all initial spectra conditions.

	$2s$ = 2		n_β = 2		n_β = 8	
γ	B	$D_{\max}$	B	$D_{\max}$	B	$D_{\max}$
1.0	0.358	0.988	0.328	1.31	0.330	1.29
3.3	0.342	0.899	0.320	1.32	0.321	1.12
7.0	0.342	0.963	0.313	1.31	0.326	1.09

$$F = \begin{cases} F_1 = (n+1)\left(\dfrac{\sigma_p}{\sigma}\right)^n \exp\left[-\dfrac{n+1}{n}\left(\dfrac{\sigma_p}{\sigma}\right)^n\right] & \text{for } \sigma \le \sigma_\pi \\ F_2 = (n+1)\left(\dfrac{\sigma_p}{\sigma}\right)^n \left(\dfrac{\sigma_\pi}{\sigma}\right)^{n_\pi - n} \exp\left[-\dfrac{n+1}{n}\left(\dfrac{\sigma_p}{\sigma_\pi}\right)^n\right] & \text{for } \sigma > \sigma_\pi, \end{cases} \tag{17}$$

where n and n_π are new nondimensional parameters that are functions of the nondimensional value $A\sigma_p/E$. As shown by the numerical results, the value n is estimated as $n = 6.0 \pm 1.0$ and $n_\pi \approx n/2$. Note that integrating the spectrum Eq. (15) with Eq. (17) within the frequency range results in the total energy value E, which is equal to

$$E = m_0\left\{1 + \frac{n+1}{n}\left(\frac{\sigma_p}{\sigma_\pi}\right)^n\left(\frac{n}{n_\pi} - 1\right) \times \exp\left[-\frac{n+1}{n}\left(\frac{\sigma_p}{\sigma_\pi}\right)^n\right]\right\}, \tag{18}$$

where $m_0 = \int_0^\infty \sigma^{-1}F_1(\sigma)\,d\sigma$.

To estimate the value n, the total wave action A can be defined as a spectrum moment of the -1 power:

$$A = m_{-1} = \int_0^\infty \sigma^{-1}S(\sigma)\,d\sigma = m_0\sigma_p^{-1}\left\{\left(\frac{n+1}{n}\right)^{-1/n}\Gamma\left(1+\frac{1}{n}\right) + \left(\frac{\sigma_p}{\sigma_\pi}\right)^{n+1}\left(\frac{n-n_\pi}{n_\pi+1}\right)\exp\left[-\frac{n+1}{n}\left(\frac{\sigma_p}{\sigma_\pi}\right)^n\right]\right\}, \tag{19}$$

where $\Gamma(n)$ is the gamma function.

Thus, the nondimensional value $A\sigma_p/E$ can be written as follows:

$$\frac{A\sigma_p}{E} = \frac{\left\{\left(\dfrac{n+1}{n}\right)^{-1/n}\Gamma\left(1+\dfrac{1}{n}\right) + \left(\dfrac{\sigma_p}{\sigma_\pi}\right)^{n+1}\left(\dfrac{n-n_\pi}{n_\pi+1}\right)\exp\left[-\dfrac{n+1}{n}\left(\dfrac{\sigma_p}{\sigma_\pi}\right)^n\right]\right\}}{\left\{1 + \dfrac{n+1}{n}\left(\dfrac{\sigma_p}{\sigma_\pi}\right)^n\left(\dfrac{n}{n_\pi} - 1\right)\exp\left[-\dfrac{n+1}{n}\left(\dfrac{\sigma_p}{\sigma_\pi}\right)^n\right]\right\}}. \tag{20}$$

It can be estimated that $A\sigma_p^0/E \approx 0.8572$ for the JONSWAP initial spectrum with its peakness of $\gamma = 1.0$ and $n = 4$. The value σ_p/σ_p^0 as a function of n_π is presented in Fig. 11.

Self-similar analytical spectrum approximation Eq. (15) with Eqs. (17) and (20) is shown in Fig. 12 for different stages of evolution. It is seen that the spectrum consists of two main domains: an energy-containing range, $0.5\sigma_p < \sigma < 1.5\sigma_p$, and a slowly decreasing tail, $\sigma > 1.5\sigma_p$.

Another useful relationship is coming from the fact that the parameter B is approximately equal to 1/3. It can be written as

$$E = \frac{S_p\sigma_p}{3} = m_0\frac{n+1}{3}\exp\left(-\frac{n+1}{n}\right). \tag{21}$$

Using Eq. (18), it can be estimated that $n \approx 7$. This value is in correspondence with the above-obtained numerical estimations.

This estimation corresponds to the numerical results obtained earlier in this paper. So, it can be assumed that Eq. (16) with Eqs. (17)–(20) describes the intermediate self-similar approximation of the frequency spectrum. It preserves the total energy and the wave action.

5. Discussion

As shown by the numerical results, some general spectra features are established in the process of the nonlinear evolution. There are two main domains: a sharply defined peak and a slowly decreasing high-frequency tail. In the low-frequency range $\sigma < \sigma_p$, the spectrum grows quickly, being approximated by the dependence $S(\sigma) \sim \sigma^{16.0\pm1.0}$. Within the range $\sigma_p < \sigma < 1.5\sigma_p$, the spectrum is decreased and approximated as $S(\sigma) \sim \sigma^{-6.5\pm0.5}$. The frequency spectrum slowly decreases as $S(\sigma) \sim \sigma^{-3.1\pm0.6}$ at the high-frequency range $\sigma > 1.5\sigma_p$. Using the obtained numerical results, a simplified intermediate self-similar frequency spectrum approximation is proposed. The approximation describes the main features of the nonlinear spectrum evolution and provides a preservation of the total energy and wave action.

To provide a physical explanation of the obtained results, note that the frequency spectrum of swell, prop-

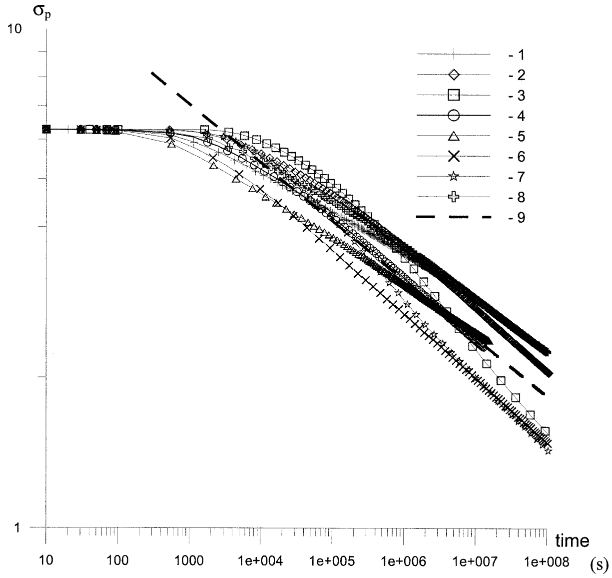

FIG. 9. Frequency maximum evolution in time for different initial spectra parameters (logarithmic scale): 1) $\gamma = 3.3$, angular distribution $\cos^8\beta$; 2) $\gamma = 1.0$, angular distribution $\cos^2\beta$; 3) $\gamma = 1.0$, angular distribution $\cos^2(\beta/2)$; 4) $\gamma = 3.3$, angular distribution $\cos^2\beta$; 5) $\gamma = 7.0$, angular distribution $\cos^8\beta$; 6) $\gamma = 7.0$, angular distribution $\cos^2\beta$; 7) $\gamma = 3.3$, angular distribution $\cos^2(\beta/2)$; 8) $\gamma = 1.0$, angular distribution $\cos^8\beta$; and 9) approximation $\sigma_{\max} = 15.85t^{-0.117}$.

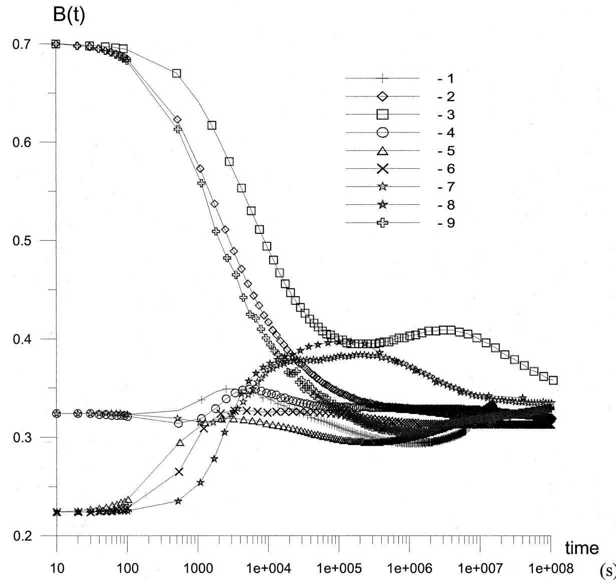

FIG. 10. Same as Fig. 9, but for parameter B time evolution for different initial spectra and for 8) $\gamma = 7.0$, angular distribution $\cos^2(\beta/2)$ and 9) $\gamma = 1.0$, angular distribution $\cos^8\beta$.

agated from a distant storm, can be approximated as follows: $S(\sigma) \approx m_0(n + 1)(\sigma_p/\sigma)^n 1/\sigma \exp[(n + 1/n)(\sigma_p/\sigma)^n]$, (where m_0 is a zero moment of the spectrum) with $n \geq 5$ (Davidan et al. 1985). So, for $\sigma > \sigma_p$, the spectrum can be estimated as $S(\sigma) \sim 1/\sigma^{n+1}$. There is a good correlation between theoretical and experimental results within the main frequency domain ($\sigma_p < \sigma < 1.5\sigma_p$) containing more than 90% of the total energy. Thus, it is possible to conclude that the field swell spectrum preserves a stable form because of nonlinear energy transfer.

There is some difference between theoretical and experimental results in the frequency range $\sigma > 1.5\sigma_p$, with the theoretical frequency spectrum being slowly decreased, providing preservation of the total energy and wave action. This discrepancy can be explained by the fact that high-frequency dissipation is not taken into account in numerical simulations.

As shown in a weak turbulence wind-wave theory, the Kolmogorov–Zakharov spectra are established because of nonlinear energy transfer (Zakharov and Zaslavskii 1982). The spectra are approximated by the power law $S(\sigma) \sim \sigma^{-x}$. The spectrum with $x = 4$ is realized in the case of constant energy flux directed from low to high frequency. The flux is provided by energy source input located at the low-frequency range and by dissipation located at the high-frequency range. In another case, if wave action flux is directed from high to low frequency, the spectrum is approximated as $S(\sigma) \sim \sigma^{-11/3}$.

Note that in our case, it is not quite so. The results presented in this paper are obtained as a solution of the kinetic equation with only nonlinear energy transfer, that is, without any wave energy input and dissipation. This solution preserves the total energy, action, and momentum of the wave system, but there are no appropriate constant fluxes as in the case of the Zakharov–Kolmogorov spectrum.

6. Conclusions

The problem of nonlinear spectral evolution based on the Hasselmann equation is solved for a large evolution time. The numerical results reveal some general features common for all cases of the spectrum evolution at large evolution time. They are as follows.

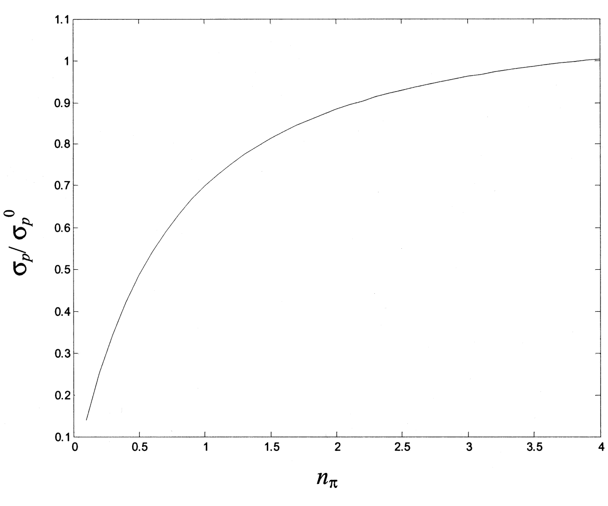

FIG. 11. Values of σ_p/σ_p^0 as a function of n_π.

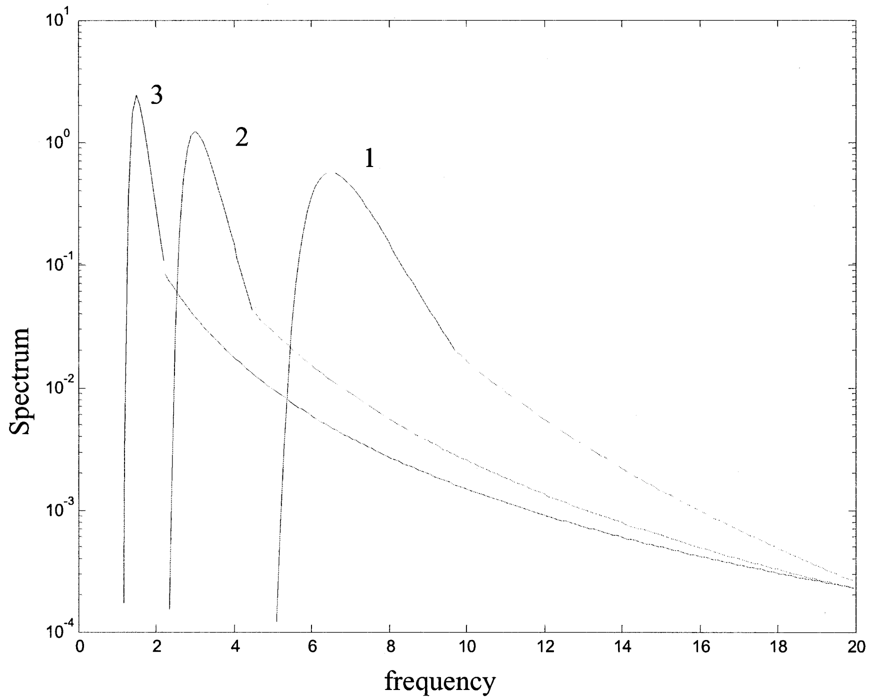

FIG. 12. Analytical self-similar spectrum approximation for the following stages: $\tilde{t}$ = 1) 10^3, 2) 10^5, and 3) 10^7.

1) An impact of the nonlinear energy transfer for all frequency–angular spectra approaches (in time) some general forms depending on the initial integral values: wave energy action and momentum.
2) The most definite features are revealed for frequency spectrum $S(\sigma)$ and function of the angular narrowness $D(\sigma)$.
3) The spectrum grows quickly in the low-frequency range $\sigma < \sigma_p$, being approximated by the dependence $S(\sigma) \sim \sigma^{16.0\pm1.0}$, whereas within the range $\sigma_p < \sigma < 1.5\sigma_p$, the spectrum is decreased and is approximated as $S(\sigma) \sim \sigma^{-6.5\pm0.5}$.
4) The frequency spectrum slowly decreases as $S(\sigma) \sim \sigma^{-3.1\pm0.6}$ at the high-frequency range $\sigma > 1.5\sigma_p$, with the frequency power depending on the angular energy distribution of the initial spectrum, the wider initial angular distribution giving a larger negative value of the power, so the isotropic initial spectrum providing the frequency dependence as $S(\sigma) \sim \sigma^{-3.67}$.
5) Spectrum maximum shifts in time to a low-frequency range as $\sigma_p \sim t^{-0.11\pm0.02}$.
6) The frequency narrowness of the value B is established as 0.33 ± 0.02 (the law of 1/3) and is practically not dependent on an initial spectral form.
7) The function of the angular narrowness $D(\sigma)$ reveals a sharp maximum in the vicinity of the frequency spectral maximum, with its value becoming smaller at the low- and high-frequency ranges.
8) The maximum of the parameter D_p is established within the range $0.9 \leq D_p \leq 1.3$, depending on the initial angular narrowness $D_p(t = 0)$.

As shown by the numerical result, the self-similar spectrum is established in the process of the nonlinear evolution. It is revealed as an establishment of the parameter values B and D_p and a total form of the spectrum. There are two main domains: a sharply defined peak and a slowly decreasing high-frequency tail. Using obtained numerical results, a simplified intermediate self-similar frequency spectrum approximation is proposed. The approximation describes the main features of the nonlinear spectrum evolution and preserves the total energy and wave action.

Acknowledgments. The author is very thankful to Dr. V. Polnikov for initiating the investigation and for fruitful discussions and to V. Zakharov for showing interest in the results. The paper is supported by Projects INTAS-99-666, INTAS-01-25, INTAS-01-234, INTAS-01-2156, and the Russian Foundation for Basic Research Grant 01-05-64846.

REFERENCES

Barenblatt, G. I., 1984: *Asymptotics and Intermediate Self-similarity* (in Russian). Hydrometeoisdat, 256 pp.

Davidan, I. N., L. I. Lopatukhin, and V. A. Rozhkov, 1985: *Wind Sea in the World Ocean* (in Russian). Gidrometeoizdat, 248 pp.

Hasselmann, K., 1962: On the non-linear energy transfer in a gravity wave spectrum. Part 1. *J. Fluid Mech.,* **12,** 481–500.

——, 1963: On the nonlinear energy transfer in a gravity-wave spectrum: Conservation theorem, wave particle correspondence, irreversibility. *J. Fluid Mech.,* **15,** 273–281.

——, and Coauthors, 1973: Measurements of wind-wave growth and swell decay during the Joint North Sea Wave Project (JONSWAP). *Dtsch. Hydrogr. Z.,* **8** (Suppl. A), 1–95.

Hasselmann, S., and K. Hasselmann, 1981: A symmetrical method of computing the nonlinear transfer in a gravity wave spectrum. *J. Hamburger Geophys. Einzelschrifte,* **A52,** 138.

——, and ——, 1985: Computations and parameterizations of the nonlinear energy transfer in a gravity-wave spectrum. Part I: A new method for efficient computations of the exact nonlinear transfer integral. *J. Phys. Oceanogr.,* **15,** 1369–1377.

Komatsu, K., and A. Masuda, 1996: A new scheme of nonlinear energy transfer among wind waves: RIAM method—algorithm and performance. *J. Oceanol.,* **52,** 509–537.

Komen, G. J., L. Cavaleri, M. Donelan, K. Hasselmann, S. Hasselmann, and P. A. E. M. Janssen, 1994: *Dynamics and Modelling of Ocean Waves.* Cambridge University Press, 532 pp.

Lavrenov, I. V., 1991a: Non-linear interaction in rips spectrum. *Izv. Acad. Sci. USSR., ser. Phys. Atmos. Ocean,* **27,** 438–447.

——, 1991b: Non-linear evolution of wave spectrum in shallow water area. *Izv. Acad. Sci. USSR., ser. Phys. Atmos. Ocean,* **27,** 1373–1378.

——, 1998: *Mathematical Modelling of Wind Waves at Non-Uniform Ocean* (in Russian). Gidrometeoìzdat, 500 pp.

——, 2001: Effect of wind wave parameter fluctuation on the nonlinear spectrum evolution. *J. Phys. Oceanogr.,* **31,** 861–873.

——, and T. A. Pasechnik, 1989: Swell propagation calculation for ocean taking into account the earth's surface sphericity. *Russ. Meteor. Hydrol.,* **6,** 73–81.

——, and F. J. Ocampo-Torres, 1999: Non-linear energy generation of waves opposite to the wind direction—the wind-driven air–sea interface. *Proc. Symp. on the Wind-Driven Air–Sea Interface,* Sydney, Australia, School of Mathematics, The University of New South Wales, 141–150.

Masuda, A., 1980: Nonlinear energy transfer between wind waves. *J. Phys. Oceanogr.,* **10,** 2082–2093.

Polnikov, V. G., 1989: Calculation of non-linear energy transfer by surface gravitational waves spectrum. *Izv. Acad. Sci. USSR, ser. Phys. Atmos. Ocean,* **25,** 1214–1225.

——, 1990: Numerical study of the kinetic equation for surface gravity waves. *Izv. Acad. Sci. USSR, ser. Phys. Atmos. Ocean,* **26,** 168–176.

——, 1993: Numerical formation of flux spectrum of surface gravity waves. *Izv. Acad. Sci. USSR, ser. Phys. Atmos. Ocean,* **29,** 1214–1225.

——, 1999: Numerical study of the equation of non-linear swell in the directional approximation. *Izv. Acad. Sci. USSR, ser. Phys. Atmos. Ocean,* **35,** 364–370.

Resio, D., and W. Perrie, 1991: A numerical study of non-linear energy flux due to wave–wave interaction. Part 1. Methodology and basic results. *J. Fluid Mech.,* **223,** 603–629.

Snyder, R. L., W. C. Thacker, K. Hasselmann, S. Hasselmann, and G. Barzel, 1993: Implementation of an efficient scheme for calculating nonlinear transfer from wave–wave interactions. *J. Geophys. Res.,* **98,** 14 507–14 525.

Snodgrass, F. E., G. W. Groves, K. Hasselmann, G. R. Miller, W. H. Munk, and W. H. Powers, 1966: Propagation of ocean swell across the Pacific. *Philos. Trans. Roy. Soc. London,* **259A,** 256–271.

Tolman, H. L., 1992: Effects of numerics on the physics in a third-generation wind-wave model. *J. Phys. Oceanogr.,* **22,** 1095–1111.

WAMDI Group, 1988: The WAM model—a third generation ocean wave prediction model. *J. Phys. Oceanogr.,* **18,** 1775–1810.

Webb, D. J., 1978: Non-linear transfer between sea waves. *Deep-Sea Res.,* **25,** 279–298.

Zakharov, V. E., 1968: Stability of periodic waves of final amplitude on a deep liquid surface. *Prikl. Mekh. Tekh. Fiz.,* **2,** 86–94.

——, and N. N. Filonenko, 1966: The energy spectrum for stochastical oscillation of fluid surface. *Dokl. Akad. Nauk SSSR,* **170,** 1292–1295.

——, and A. V. Smilga, 1981: About quasi-one–dimensional spectrum of weak turbulence. *J. Exp. Tekh. Fiz.,* **18,** 1318–1326.

——, and M. M. Zaslavskii, 1982: The kinetic equation and Kolmogorov's spectra in the weakly turbulent theory of wind waves. *Izv. Acad. Sci. USSR, ser. Phys. Atmos. Ocean,* **18,** 970–979.

——, and ——, 1983: Dependence of wave parameters on wind speed, duration of its action, and fetch in a weakly-turbulent theory of wind waves. *Izv. Acad. Sci. USSR., ser. Phys. Atmos. Ocean,* **19,** 406–416.

Zaslavskii, M. M., 1989: About narrow directional approach of the kinetic equation for wind wave. *Izv. Acad. Sci. USSR, ser. Phys. Atmos. Ocean,* **25,** 402–410.

——, 2000: Non-linear evolution of swell spectrum. *Izv. Acad. Sci. USSR, ser. Phys. Atmos. Ocean,* **36,** 275–283.